Relativistic photoionization cross sections for C II

Sultana N. Nahar
Department of Astronomy, The Ohio State University, Columbus, Ohio 43210
(Received 20 June 2001; published 15 April 2002)

The first measurement of highly resolved photoionization cross sections of the ground state of C II was reported recently by Kjeldsen *et al.* [Astrophys. J. **524**, L143 (1999)]. The observed resonance features showed good agreement with the theoretical calculations in the close-coupling approximation [S. Nahar, Astrophys. J. Suppl. Ser. **101**, 423 (1995)]. However, there were several observed resonances that were missing in the theoretical predictions. The earlier theoretical calculation was carried out in LS coupling where the relativistic effects were not included. Present paper reports photoionization cross sections including relativistic effects in the Breit-Pauli R-matrix (BPRM) approximation. The configuration interaction eigenfunction expansion for the core ion C III consists of 20 fine-structure levels dominated by the configurations from $1s^22s^2$ to $1s^22s3d$. Detailed features in the calculated cross sections exhibit the missing resonances due to fine structure. The results provide a benchmark for the accuracy of BPRM photoionization cross sections, as needed for the recent and ongoing experiments for high-resolution photoionization cross sections at synchrotron-radiation sources.

DOI: 10.1103/PhysRevA.65.052702 PACS number(s): 32.80.Fb

I. INTRODUCTION

Although a large number of theoretical calculations for photoionization cross sections have been carried out, the data have not yet been sufficiently calibrated against the new generation of high-resolution experiments. We refer, in particular, to the calculations using the close-coupling R-matrix method extensively utilized in the Opacity Project (OP) [1], the Iron Project (IP) [2] and similar works that accurately consider the numerous autoionizing resonances in cross sections along interacting (overlapping) Rydberg series. Most of the vast amount of photoionization data computed under the OP, IP, and other works, is estimated to be accurate to 10–20 %. However, no detailed comparisons with experiments have been possible since photoionization cross sections were not measured with equally detailed features. However, resonances can now be finely resolved in recent experiments being carried out with synchrotron-radiation sources in Refs. [3–5]. Comparing the theoretical calculations with experiments is therefore of considerable current importance. Furthermore, the quality of experimental work is such as to clearly delineate the fine structure, necessitating the inclusion of relativistic effects in an *ab initio* manner. In this report we present such a comparison between theory and experiments in detail.

Carbon is one of the most cosmically abundant elements, and C II is an important ion in astrophysical sources, such as the interstellar medium. Study of accurate features of C II is of considerable interest and important for accurate spectral analysis. In their merged ion-photon beam experiment, Kjeldsen *et al.* [3] measured the first detailed photoionization cross sections (σ_{PI}) of C II with high accuracy. With the synchrotron-radiation from an undulator, their measurements exhibited highly resolved features of autoionizing resonances in cross sections. The features agreed very well with the results from close-coupling approximation using the R-matrix method [6]. However, the theoretical calculations did not include the relativistic effects and therefore did not predict the observed fine structure features.

Extensive earlier works, such as the Opacity Project, were carried out in LS coupling and did not consider the fine structure. The motivation for the present work is to study relativistic effects in relation to the observed features using the Breit-Pauli R-matrix (BPRM) method [7,2,8]. The method has been extended to a self-consistent treatment of photoionization and electron-ion recombination (e.g., [9]). The total recombination cross sections, derived from photoioization cross sections, in an unified treatment have been extensively compared with measured recombination spectra [9,10]. The recombination cross sections require total contributions from photoionization cross sections of all bound levels. The present work, on the other hand, focuses on individual features of photoionization cross sections of the fine-structure levels of the ground configuration $2s^22p$ of C II, in direct comparision with measured cross sections.

II. THEORY AND CALCULATIONS

The calculations for photoionization cross sections (σ_{PI}) are carried out in the close-coupling approximation using the Breit-Pauli R-matrix method in intermediate coupling. Photoionization is described in terms of an eigenfunction expansion over coupled levels of the residual (''core'' or ''target'') ion. The total wave function of the $(N+1)$-electron ion is represented by the wave functions of the N-electron core, multiplied by the wave function of the outer electron as follows:

$$\Psi_E(e+\text{ion}) = A\sum_i \chi_i(\text{ion})\,\theta_i + \sum_j c_j \Phi_j(e+\text{ion}), \tag{2.1}$$

where χ_i is the target wave function in a specific state $S_iL_i\pi_i$ or level $J_i\pi_i$ and θ_i is the wave function for the $(N+1)$ th electron in a channel labeled $S_iL_i(J_i)\pi_i k_i^2 l_i(J\pi)$; k_i^2 is its incident kinetic energy. Φ_j's are the correlation functions of the $(N+1)$-electron system that account for short-range correlation and the orthogonality between the continuum and bound orbitals. The complex resonant structures in photoionization are included through channel couplings.

TABLE I. Energy levels of C III in the eigenfunction expansion of C II. The list of spectroscopic and correlation configurations, and the scaling parameter (λ) for each orbital are given as follows. Spectroscopic: $2s^2$, $2s2p$, $2p^2$, $2s3s$, $2s3p$, $2s3d$; correlation: $2p3s$, $2p3p$, $2p3d$, $3s3p$, $3s3d$, $2s4s$, $2s4p$, $4s4p$; λ: 1.42(1s),1.4(2s),1.125(2p),1.(3s),1(3p),1(3d),3.3(4s),3(4p).

	Level		E (Ry)
1	$2s^2$	$^1S_0$	0.
2	$2s2p$	$^3P^o_2$	0.47793
3	$2s2p$	$^3P^o_1$	0.4774
4	$2s2p$	$^3P^o_0$	0.4772
5	$2s2p$	$^1P^o_1$	0.9327
6	$2p^2$	$^3P_2$	1.2530
7	$2p^2$	$^3P_1$	1.2526
8	$2p^2$	$^3P_0$	1.2523
9	$2p^2$	$^1D_2$	1.3293
10	$2p^2$	$^1S_0$	1.6632
11	$2s3s$	$^3S_1$	2.1708
12	$2s3s$	$^1S_0$	2.2524
13	$2s3p$	$^1P^o_1$	2.3596
14	$2s3p$	$^3P^o_2$	2.3668
15	$2s3p$	$^3P^o_1$	2.3667
16	$2s3p$	$^3P^o_0$	2.3666
17	$2s3d$	$^3D_3$	2.4606
18	$2s3d$	$^3D_2$	2.4605
19	$2s3d$	$^3D_1$	2.4605
20	$2s3d$	$^1D_2$	2.5195

Relativistic effects are included through Breit-Pauli approximation in intermediate coupling. The Breit-Pauli Hamiltonian, as adopted in the IP work [2], is

$$H^{\rm BP}_{N+1}=H_{N+1}+H^{\rm mass}_{N+1}+H^{\rm Dar}_{N+1}+H^{\rm so}_{N+1}, \qquad (2.2)$$

where H_{N+1} is the nonrelativistic Hamiltonian,

$$H_{N+1}=\sum_{i=1}^{N+1}\left\{-\nabla_i^2-\frac{2Z}{r_i}+\sum_{j>i}^{N+1}\frac{2}{r_{ij}}\right\}, \qquad (2.3)$$

and the additional terms represent the one-body mass correction term, the Darwin term, and the spin-orbit interaction term, respectively.

Present wave functions for C II are expressed by a 20-level expansion of the core ion C III with configurations $2s^2,2s2p,2p^2,2s3s,2s3p,2s3d$ (the K shell is closed) (Table I). The C III wave functions were obtained from atomic structure calculations using a scaled Thomas-Fermi model in the code SUPERSTRUCTURE [11]. The spectroscopic and correlation configurations, and the scaling parameters in the Thomas-Fermi potential for the orbitals, are given in Table I. The correlation term in Eq. (2.1) considers all possible $(N+1)$-electron configurations up to $2p^3,3s^2,3p^2,3d^2,4s^2,4p^2$.

The computations of σ_{PI} are carried out using the package of BPRM codes from the Iron Project [8]. The cross sections are computed with a very fine energy mesh in order to delineate the detailed resonance structures as observed in the experiments. It is a computationally demanding procedure because of repeated computations with exceedingly fine energy bins to search and resolve the resonances. Many resonances are sharp and narrow, and cannot be detected individually in the experiment. The resonances are convolved with a Gaussian function of full width at half-maximum (FWHM) equal to the energy bandwidth of the monochrometer in the experiment.

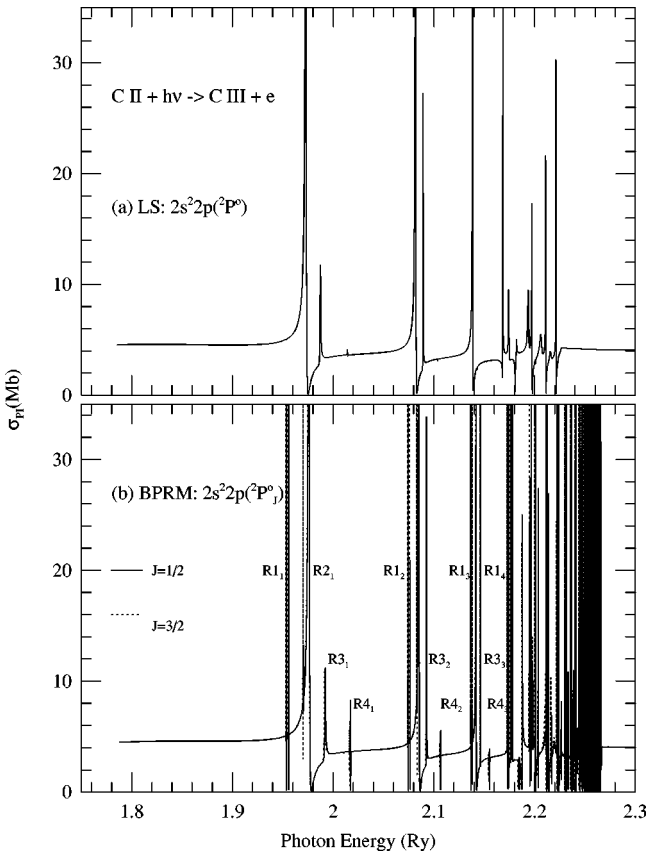

FIG. 1. Photoionization cross sections σ_{PI} of the (a) ground $2s^22p(^2P^o)$ state in LS coupling, and (b) levels $^2P^o_J$, where $J=1/2$ (solid curve) and 3/2 (dotted curve) in BPRM intermediate coupling, of ground configuration of C II.

III. RESULTS AND DISCUSSIONS

Photoionization cross sections are obtained for the fine-structure levels of the ground state, $2s^22p(^2P^o_{1/2,3/2})$, and of the metastable state, $2s2p^2(^4P_{1/2,3/2,5/2})$ of C II. The fine-structure features are distinct when compared with those in LS coupling. σ_{PI} for the ground state obtained in nonrelativistic LS coupling are presented in Fig. 1(a) and in relativistic BPRM approximation in Fig. 1(b), the solid curve for the $^2P^o_{1/2}$ level and the dotted curve for the $^2P^o_{3/2}$.

The relativistic σ_{PI} for the levels $^2P^o_{1/2}$ and $^2P^o_{3/2}$ show many overlapping resonances. The number of resonances is considerably larger in the bottom panel than that for the ground $^2P^o$ state in the LS coupling in the top panel. Inclusion of relativistic effects in the BPRM approximation intro-

duces more Rydberg series of resonances, belonging to the increased number of core ion thresholds through fine-structure splitting, in comparison with nonrelativistic LS coupling calculations. For example, the 12 LS terms of the core ion C III correspond to 20 fine-structure levels. Additional thresholds and associated resonances, allowed in intermediate coupling but not in LS coupling, have resulted in more extensive resonances.

The first two resonances in σ_{PI} in LS coupling [Fig. 1(a)] belong to the Rydberg series of autoionizing states $2s2p(^3P^o)np(^2D)$ and $2s2p(^3P^o)np(^2S)$, respectively, where $n=4$. A Rydberg series may be identified by the quantum defects. The effective quantum number number ν of an autoionizing state can be obtained from the quantum-defect formula, $\nu=z/\sqrt{(E-E_T}$, where z is the ion charge, E is the resonance energy, and E_T is the threshold energy in Rydbergs. Given that $n=\nu+\mu$, the quantum defect μ is ≈ 0.6 for an s electron, ≈ 0.4 for a p electron, ≈ 0.1 for a d electron, and so on. The above-mentioned two series of resonances are are allowed in LS coupling and are common in both panels of Fig. 1, denoted as $R2$ and $R3$ series in the BPRM σ_{PI} [Fig. 1(b)]. Photoionization of the ground state $2s^22p(^2P^o)$ is allowed to the even parity ^2S and ^2D continua, but not to ^2P, in LS coupling. The autoionizing states $2s2p(^3P^o)np(^2P)$ cannot decay via a radiationless transition to the $2s^2(^1S)\epsilon l$ continuum with the same symmetry ^2P. However, all three Rydberg series of resonances, $2s2p(^3P^o)np(^2S,^2P,^2D)$, converging on to the thresholds of $2s2p(^3P^o)$ are allowed in relativistic intermediate coupling (IC). The sharp, narrow $R1$ series of resonances in the BPRM cross sections in Fig. 1(b) correspond to $2s2p(^3P^o)np(^2P)$ states. The channel couplings for the $J=1/2$ level mixes $^2S_{1/2}$ with a component of $^2P_{1/2}$, and for the $J=3/2$ level mixes $^2D_{3/2}$ with $^2P_{3/2}$ through IC, and thus enable the symmetry ^2P to autoionize. Indirect decay to ^2P continuum via radiative decay first to, for example, $2s2p(^3P^o)3d(^2P)$ state followed by autoionization is possible, but not likely to be significant [3].

The $R4$ series of resonances in Fig. 1(b), which could be identified as the combination of states $2s2p(^1P^o)np(^2D,^2P,^2S)$, are also common (except for the ^2P component) to both panels in Fig. 1. These resonances are weak, especially in LS coupling calculations, partially due to coarser energy mesh in the previous work. Our identification of this series differs from that of Kjeldsen *et al.* [3]. This series was not observed in the experiment. Additional series of resonances are introduced starting from the fourth complex, which overlap with other complexes. Small shifts in the energies of resonances seen in the upper and lower panels of Fig. 1 are due to statistical averaging of LS term energies over their fine-structure components.

The BPRM photoionization cross sections are compared with the measured cross sections by Kjeldson *et al.* after convolution of the calculated resonances with a Gaussian distribution function of FWHM of 35 meV, the monochrometer bandwidth of the experiment. The calculated ionization energy for the $^2P^o_{1/2}$ ground level is 1.7885 eV, compared to the measured energy of 1.7921 eV; for the $^2P^o_{3/2}$ level it is

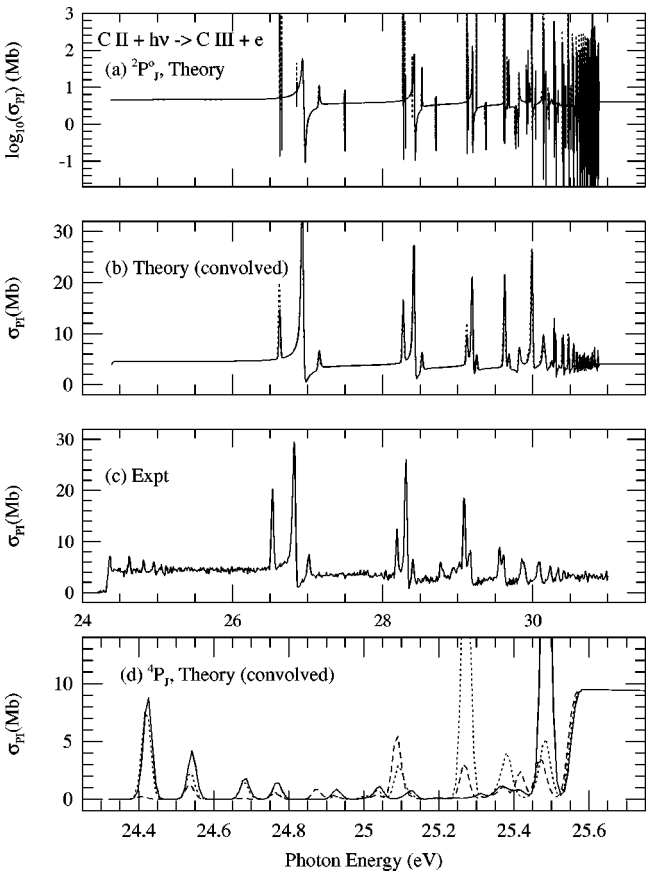

FIG. 2. Photoionization cross sections σ_{PI} of C II (a) detailed with resonances of levels $^2P^o_{1/2}$ (solid) and $^2P^o_{3/2}$ (dotted) of ground configuration $1s^22s^22p$, (b) the same cross sections convolved with monochrometer bandwidth of the experiment, (c) experimentally measured cross sections by Kjeldsen *et al.*, (d) convolved cross sections of excited levels $2s2p^2(^4P_J)$, $J=1/2$ (solid), $J=3/2$ (dotted), $J=5/2$ (dashed).

1.78 793 eV compared to the measured value 1.7916 eV. Calculated cross sections have been slightly shifted to the measured ionization thresholds to compare with the experimenally measured σ_{PI}, as shown in Fig. 2.

Figure 2(a), presents the total detailed calculated cross sections of the levels $^2P^o_{1/2,3/2}$ (solid and dotted curves, respectively), while Fig. 2(b) presents the convolved σ_{PI} on the eV scale. Fig. 2(c) presents the measured cross sections [3]. Very good agreement is seen, in general, in resonance features between the calculations [Fig. 2(b)] and the measurements [Fig. 2(c)]. The resonance peaks are also in good agreement in the first three resonance complexes. However, some differences are noted for the higher complexes. Peaks of some calculated resonances at higher energies are higher than the measured ones. The peaks may be reduced by radiative decays or the process of dielectronic recombination. The peak values were checked by including the radiation damping effect, with no significant reduction. This is expected for a low-charge carbon ion since the radiative decay rates of the excited core thresholds ($\approx 10^8$,10^9 sec^{-1}) are several orders of magnitude lower than typical autoionization rate ($\approx 10^{13-14}$ sec^{-1}), thus causing very little damping. How-

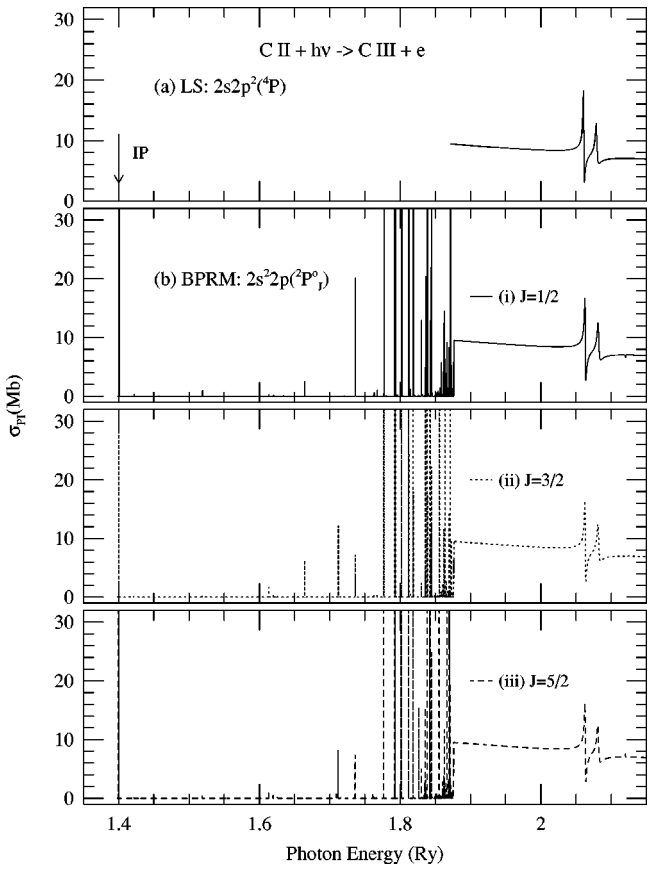

FIG. 3. Photoionization cross sections of the first excited $2s2p^2(^4P)$ state of C II (a) in LS coupling, (b) of levels (i) $J=1/2$, (ii) $J=3/2$, and (iii) $J=5/2$ in BPRM approximation. The arrow points to the ionization threshold for the fine-structure levels.

ever, some explanation can be given for the differences. Although Gaussian averaging of resonances has shown good agreement with the measured cross sections, as carried out in the present case and shown by the experimental group [3], the distribution may not be adequate throughout the energy range. The same FWHM may not remain constant with energies. A convolved peak can be flatteneed with a larger bandwidth. Also, resonances become narrower and denser as the energy approaches the convergent threshold, requiring a narrower bandwidth monochrometer for finer resolution. To see the structures at higher energies near the highest C III threshold, the calculated resonances beyond 30.2 eV are convolved with a narrower FWHM, and hence seem sharper than the measured cross sections.

Photoionization cross sections of the three fine-structure levels, $J=1/2,3/2$, and $5/2$, of the first excited (metastable) state $2s2p^2(^4P)$ of C II are presented in Figs. 2(d) and 3. Figure 2(d) presents the convolved cross sections for excited $2s2p^2(^4P_J)$ levels in a small energy region, from 24.2 eV to about 25.5 eV, while Fig. 3 presents the detailed cross sections over a wider range of energy. Kjeldsen *et al.* [3] found a few resonances from photoionization of ^4P levels in the near threshold energy region of $^2P^o$ photoionization, indicating the presence of a mixture of $^2P^o$ and ^4P states in the C II experimental beam in the low-energy region. They identified the resonances to belong mainly to nd series, i.e., to $2s2pnd$ $(n=7,8,\ldots)$ rather than to ns series, since the transition rates to the higher l are usually more dominant. However, transitions to $2s2pns$ states are also possible. These observed resonances are seen in the BPRM σ_{PI}. However the convolved resonance peaks are relatively lower, except for the first one, compared to observations. Resonances in this energy region are extremely narrow; further resolution could conceivably have improved agreement with the measured ones.

Photoionization cross sections of ^4P state in LS coupling are presented in Fig. 3(a) (top panel) for comparison. No cross sections can be seen below the threshold at 1.872 Ry, photoionizing to $2s2p(^3P^o)$ state of C III. However, in the σ_{PI} for the fine-structure levels $^4P_{1/2,3/2,5/2}$, shown separately as solid, dotted, and dashed curves in Fig. 3, extensive narrow resonances are seen below this threshold with almost no background. The ionization thresholds for these levels lie at about 1.4 Ry (pointed by arrow in the figure), and each level exhibits presence of a near threshold resonance. As explained above, these resonances are allowed by relativistic mixing of states through IC. For example, IC allows $J\pi=1/2^o$ and $3/2^o$ levels of autoionizing states $2s2p(^3P^o)nd(^4D^o)$ to decay to $J\pi=1/2^o$ and $3/2^o$ of continuum $2s^2(^1S)\epsilon p(^2P^o)$ via radiationless transitions. As we are mainly interested in the energy region corresponding to photoionization of the ground state of C II, resonances in photoionization of the levels $J=1/2,3/2,5/2$ are resolved with a much finer energy mesh from ≈ 1.75 Ry to about 1.87 Ry, and are convolved with the same monochrometer bandwidth of 35 meV and are presented in Fig. 2(d) for comparison with the measured cross sections.

IV. CONCLUSION

We have demonstrated that the theoretical fine structure photoionization cross sections account for nearly all experimentally observed features that may not be obtained in the nonrelativistic LS coupling calculations. The relativistic BPRM σ_{PI} of the ground $2s^22p(^2P^o)$ state and the first excited $2p2p^2(^4P)$ state of C II reveal the fine structure observed in the experiment [3] and are in very good agreement. Convolution of detailed resonances may result in some variations of peaks depending on the monochrometer bandwidth, choice of energy distribution function, and resolution of resonances.

Similar to the experimental work by Kjeldsen *et al.* [3], Phaneuf *et al.* [12] plan collaborative measurements on C II with the Aarhus group at higher resolutions using a different setup at the ALS (Advance Light Source). Cross-section values from the present work are available electronically for comparison with other experiments.

ACKNOWLEDGMENTS

This work was partially supported by the National Science Foundation and the NASA Astrophysical Theory Program. The computational work was carried out at the Ohio Supercomputer Center.

[1] *The Opacity Project 1 & 2*, compiled by the Opacity Project team (Institute of Physics, London, UK, 1995, 1996).
[2] D.G. Hummer, K.A. Berrington, W. Eissner, A.K. Pradhan, H.E. Saraph, and J.A. Tully, Astron. Astrophys. **279**, 298 (1993).
[3] H. Kjeldsen, F. Folkmann, J.E. Hensen, H. Knudsen, M.S. Rasmussen, J.B. West, and T. Andersen, Astrophys. J. **524**, L143 (1999) (the experimental data were obtained through private communication).
[4] A.M. Covington, A. Aguilar, I.R. Covington, M. Gharailbeh, C.A. Shirley, R.A. Phaneuf, I. Alvarez, C. Cisneros, G. Hinojosa, J.D. Bozek, I. Dominguez, M.M. Sant'Ama, A.S. Schlachter, N. Berrah, S.N. Nahar, and B.M. McLaughlin, Phys. Rev. Lett. **87**, 243002 (2001).
[5] J.-M. Bizau *et al.*, Phys. Rev. Lett. **84**, 435 (2000).
[6] S.N. Nahar, Astrophys. J., Suppl. Ser. **101**, 423 (1995).
[7] N.S. Scott and K.T. Taylor, Comput. Phys. Commun. **25**, 347 (1982); N.S. Scott and P.G. Burke, J. Phys. B **12**, 4299 (1980).
[8] K.A. Berrington, W. Eissner, and P.H. Norrington, Comput. Phys. Commun. **92**, 290 (1995).
[9] H.L. Zhang, S.N. Nahar, and A.K. Pradhan, J. Phys. B **32**, 1459 (1999).
[10] A.K. Pradhan, S.N. Nahar, and H.L. Zhang, Astrophys. J. Lett. **549**, L265 (2001).
[11] W. Eissner, M. Jones, and N. Nussbaumer, Comput. Phys. Commun. **8**, 270 (1974).
[12] R. Phaneuf *et al.* (private communication).